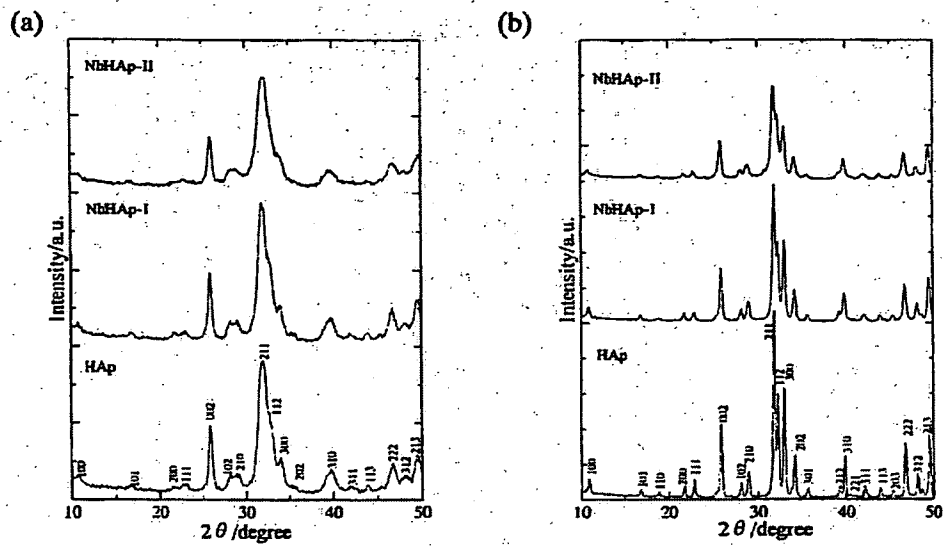

Fig.1. XRD patterns of HAp and NbHAp-I and NbHAp-II before (a) and after (b) annealing(800°C, 2h).

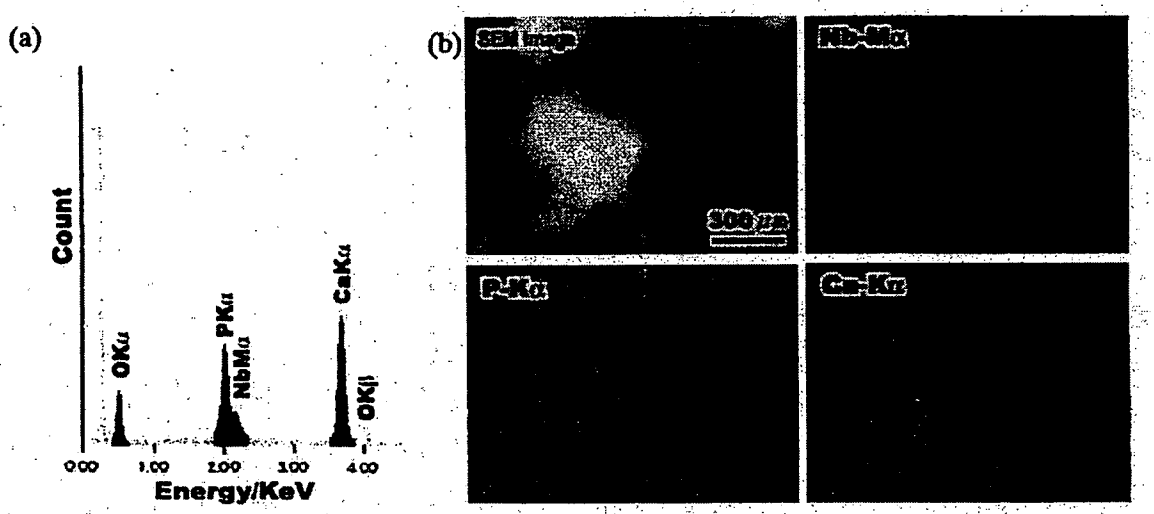

Fig.2. SEM-EDX analysis of NbHAp-II. ((a) An EDX spectrum and (b) SEM image and element mapping images of Nb, Ca and P).

As shown in Table1, the Nb/(Nb+P) molar ratio of NbHAp-I and NbHAp-II were 0.015 and 0.082, respectively. SEM observation revealed that the precipitates were present as aggregates composed of primary particles of less than 1μm in diameter.

XRD patterns of NbHAps annealed at 800°C are shown in Fig.1(b). The crystalline of the precipitates become high by the annealing and XRD patterns of all annealed NbHAps could be identified as monolithic apatitic structure. It is noted that the crystallite of the NbHAp decreased as Nb content increased. Figure 2(a) shows an EDX spectra of the whole region of SEM image in Fig.2(b). The EDX spectrum from Nb M_α was separated from P K_α line and could be observed at 2.17KeV, although the intensity of the spectra was weak. The mapping image of Nb, Ca and P ions are shown in Fig.2(b). As shown in Fig.2(b), Nb ions were present at the same site of Ca and P ions. Based on these observations, Nb ions are suggested to be uniformly distributed in the

aggregates. High-resolution XPS spectrum of Nb $3d_{5/2}$ of NbHAp-II annealed at 800°C is shown in Fig.3. The peak of XPS spectra due to $3d_{5/2}$ of Nb ions from annealed NbHAp-II is at 208.3eV. Since XPS peak of $3d_{5/2}$ due to Nb^{2+} from NbO and Nb^{5+} from Nb_2O_5 appears at 203.5eV and 207.2eV, respectively, the Nb ions in NbHAp can be identified as Nb^{5+}.

These results suggest that the NbHAp has apatitic structure containing Nb ions and the Nb ions are homogenously distributed in the grain. Generally, Nb^{5+} ions in the solution is not present as Nb^{5+} but as niobiumate acid, $H_xNb_6O_{19}^{(8-x)-}$ ions (X=0,1,2)[4]. The PO_4 in HAp can be replaced by anionic atomic group, e.g. CO_3^{2-}, VO_4^{3-} and AsO_4^{3-}. Therefore, it is probable that Nb ions are substituted in PO_4 site in HAp. However, measured Nb/(Nb+P) molar ratio in NbHAp-II was 0.082, despite their theoretical Nb/(Nb+P) ratio of 0.1667, suggesting that the value of the measured ratio might be the maximum amount of Nb ions in PO_4, practically.

Since Nb ions are expected to have an effect to promote the proliferation and ALP activity of osteoblastic cells, the NbHAps have a potential to promote the ALP activity of osteoblastic cells.

Figure 4 shows ALP activity of NHOst cultured with annealed NbHAps. As shown in Fig.4, NHOst cultured with the NbHAp expressed the ALP activities twice as much as that of NHOst cultured with HAp without Nb ions. It is well known that ALP is often expressed when fracture of bone is repaired *in vivo*. Furthermore, from the recent study, it has revealed that the ALP contributed to mineralization in bone formation[5]. Therefore, this enhancement in ALP activity of NHOst by NbHAp suggests that the NbHAp can promote the mineralization of bone formation.

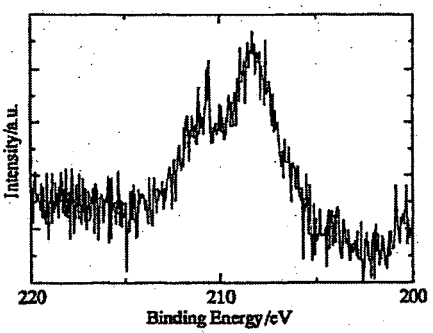

Fig.3. High-resolution XPS spectrum of Nb $3d_{5/2}$ of NbHAp-II annealed at 800°C.

Conclusion

We have succeeded to synthesize novel HAp containing Nb ions. The NbHAp would be a solid solution, which Nb ions were in PO_4 site in HAp and could enhance the ALP activity in NHOst.

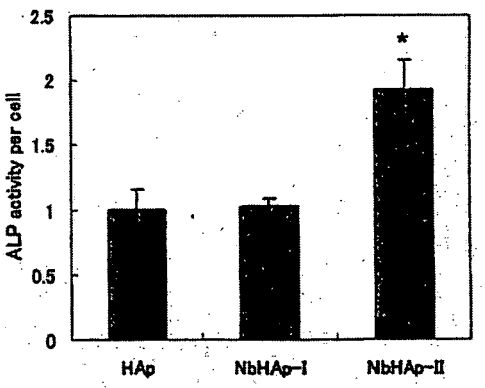

Fig.4. ALP activity of NHOst cultured with annealed NbHAp
*p<0.05 against HAp (without Nb ions)

Acknowledgment

This study was supported in part by a Grant-in-Aid for Scientific Research on Advanced Medical Technology from Ministry of Labour, Health and Welfare, Japan and a Grant-in-Aid from Japan Human Sciences Foundations.

References

[1] J.C.Elliott: *Structure and chemistry of the apatite and other calcium orthophosphates* (Elsevier, Tokyo, 1994)
[2] K.Isama, and T.Tsuchiya: Bull.Natl.Inst.Health.Sci., Vol.121 (2003) p.111
[3] T.Ohya, T.Ban, YOhya and Y.Takahashi: Ceram.Trans., Vol.112 (2001) p.47
[4] F.A.Cotton and G.Wilkinson: *Advanced Inorganic Chemistry* (Baifukan, Tokyo, 1994)
[5] H.Sowa, H.Kaji, T.Yamaguchi, T.Sugimoto and K.Ichihara: J.Bone.Miner.Res. Vol.17 (2002) p.1190

Key Engineering Materials Vols. 309-311 (May 2006) pp. 1293-1296
online at http://www.scientific.net

Enhancement of Differentiation and Homeostasis of Human Osteoblasts by Interaction with Hydroxyapatite in Microsphere Form

Ryusuke Nakaoka [a] and Toshie Tsuchiya [b]

Division of Medical Devices, National Institute of Health Sciences
1-18-1 Kamiyoga, Setagaya-ku, Tokyo 158-8501, JAPAN
[a] nakaoka@nihs.go.jp, [b] tsuchiya@nihs.go.jp

Key words: osteoblasts, differentiation, homeostasis, hydroxyapatite, biocompatibility

Abstract. The aseptic loosening of artificial joints with associated periprosthetic bone resorption may be partly due to the suppression of osteoblast function to form new bone by wear debris derived from the joint. To assess the effect of wear debris on osteoblasts, we cultured normal human osteoblasts (NHOst) in contact with several kinds of microspheres as models of wear debris. The NHOst in contact with polystyrene, polyethylene, and alumina microspheres showed a lower differentiation level than NHOst alone as estimated from the amounts of deposited calcium. On the other hand, hydroxyapatite particles enhanced the differentiation of NHOst. In addition, sintered hydroxyapatite enhanced expression of osteocalcin mRNA and gap junctional communication of NHOst. This study suggests that polystyrene, polyethylene, and alumina microspheres have the potential to disorder not only the differentiation but also the homeostasis of NHOst in contact with them. However, hydroxyapatite enhanced the differentiation as well as the homeostasis of NHOst, even in microsphere form, suggesting its good biocompatibility as biomaterials for bone tissues.

Introduction

Biomaterials implanted into the harsh environment of the body cannot maintain their original shape, or even their desired function, resulting in undesirable side effects. One good example is the aseptic loosening of artificial joints observed in many patients who underwent a total joint replacement 5 to 25 years ago. Many researchers have reported that aseptic loosening with associated periprosthetic bone resorption is partly due to the activation of macrophages and osteoclasts by wear debris from the artificial joint [1-3], but few researches have focused on the interaction between wear debris and osteoblasts, especially normal human osteoblasts [4]. In this study, normal human osteoblasts were cultured in contact with various kinds of microspheres made from polymers or ceramics used as model wear debris, and the effects of the microspheres' characteristics and interaction conditions were discussed in regard to the proliferation, differentiation and homeostasis maintenance of the osteoblasts.

Materials and Methods

Microspheres. Monodispersed polystyrene (PS) microspheres with different diameters (0.1, 0.5, 1, 5, and 10 μm) were kindly supplied by Japan Synthetic Rubber Co., Ltd. (Tokyo, JAPAN). Low-density polyethylene (PE) microspheres were kindly provided by Sumitomo Seika chemicals Co., Ltd. (Tokyo, JAPAN). Alumina (Al_2O_3) microspheres were obtained from the Association of Powder Process Industry and Engineering. Sintered and un-sintered hydroxyapatite (HAp) microspheres (7.2 μm in diameter) were prepared and supplied by Ube Material Industries, Ltd. (Chiba, Japan). Determined by Multisizer II (Coulter Electronics Inc., Hialeah, FL), the average diameters of PE and alumina microspheres were found to be 6.4 and 5.1 μm, respectively. Sterile microspheres and microsphere-coated plates were prepared by the method previously reported [5]. The obtained microspheres and microsphere-coated plates (20 μg/well) were subjected to the assays.

Cellular Assays. Normal human osteoblasts (NHOst) were purchased from BioWhitteker Inc. (Walkersville, MD). The cells were maintained using alpha minimum essential medium (Gibco) containing 20% fetal calf serum (FCS) in incubators (37°C, 5%-CO_2-95%-air, saturated humidity).

All assays were carried out using the medium supplemented with 10mM β-glycerophosphate. NHOst ($2x10^4$ cells/well/500 μl medium) were cultured on the microsphere-coated plates for estimating the effect of the microspheres from the bottom of the cells. To estimate the effect of microspheres on cells adhered to the culture plates, the NHOst were cultured with microsphere-containing medium (20 μg/500 μl medium) after they had adhered to the collagen-coated plates. The cell number ratio of NHOst cultured with microspheres was evaluated using the alamar Blue™ assay (BioSource International, Inc., Camarillo, CA), which incorporates an oxidation-reduction indicator based on the detection of metabolic activity, according to manufacturer's instruction.

The level of alkaline phosphatase (ALP) activity of the NHOst and the amounts of calcium deposited during a 7-day incubation were evaluated to estimate differentiation level of NHOst as previously reported [6]. In addition, RT-PCR was performed to detect the expression of osteocalcin mRNA in the NHOst (primers for human osteocalcin [7]; forward 5'CATGAGAGCCCTCACA3' and reverse 5'AGAGCGACACCCTAGAC3'; product size 307-bp).

Gap junctional intercellular communication (GJIC), which is a function that plays an important role in maintaining cell and tissue homeostasis by exchanging low molecular weight molecules [8], among NHOst co-cultured with microspheres were evaluated using FRAP assay as previously reported [9].

All data were expressed as the mean value ± the standard deviation (SD) or the standard error of means (SEM) of the obtained data as indicated in all figures and tables. The Fisher-Tukey criterion was used to control for multiple comparisons and to compute the least significant difference between means.

Results and Discussion

Figure 1 shows the effect of the diameter of pre-coated polystyrene microspheres on proliferation, the ALP activity of co-cultured NHOst cells, and the amounts of deposited calcium on the NHOst. To compare the effect of the microspheres on the ALP activities and the calcium amounts for each NHOst, the obtained data were standardized based on the cell number ratio co-cultured with the microspheres. As shown in figure, suppression on ALP activity of NHOst and the amounts of deposited calcium were observed when 0.1 μm and 5 μm microspheres were co-cultured. When the microspheres were added after cell adhesion, they did not show a significant inhibitory effect on the functions of NHOst (data not shown). By pre-coating of the microspheres on the bottom of the test plates, the area they occupied became larger as their diameter became smaller. This increase in the microsphere occupied area would affect many functions of the test cells, resulting in the inhibitory effect of the 0.1μm microspheres on the function of NHOst when the same quantity of microspheres was coated. On the other hand, the suppression of ALP activity of NHOst and calcium deposition by pre-coated 5 μm PS microspheres suggests that not only the area they occupied but also their size may cause the unique inhibitory activity of the 5 μm PS microspheres. It is well known that the size of a microsphere plays an important role in phagocytosis [10], although it is unclear that there is the same size dependence on phagocytosis by the NHOst as by macrophages. In addition, our previous study suggested that even fibroblasts were likely to phagocyte microspheres of a specific

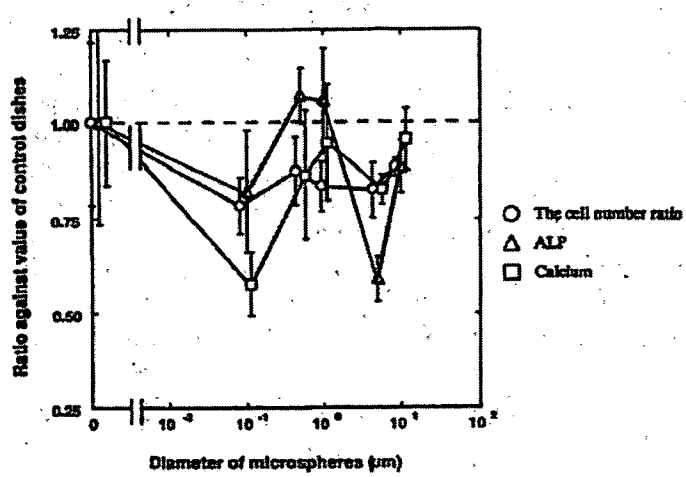

Figure 1. Effects of diameter of pre-coated PS on various functions of NHOst. Data are shown as the means±SD

diameter [5,9]. Taking into account our findings about the inhibitory effects of various microspheres on the functions of NHOst, it is probable that NHOst can phagocyte PS microspheres as well as macrophages, and in particular, may phagocyte microspheres 5 μm in diameter. Moreover, the effect of the added PS microspheres suggests that NHOst better recognize the microspheres from their lower than upper side. This may explain the reduced functions of NHOst co-cultured with the pre-coated 5 μm PS microspheres.

To estimate the effect of the material composing the microspheres, NHOst were cultured for 1 week on pre-coated PS, PE, alumina and HAp microspheres, all of which have a diameter of around 5 μm. Table 1 shows their number ratio and ALP activities, and the calcium amounts. Pre-coated PS, PE and alumina microspheres showed the potential to suppress functions of NHOst although some of these data did not show statistical differences against NHOst without microspheres. However, when NHOst were cultured with pre-coated HAp, the amount of calcium deposited was almost twice that detected in the cells without microspheres. It was observed that HAp microspheres have no potential to deposit calcium after a 1-week incubation without NHOst (data not shown). Therefore, the increase in calcium deposition by pre-coated HAp may be due to the enhancement in the differentiation of NHOst in contact with HAp. As expected, added various microspheres affected NHOst in a similar manner but less than the pre-coated microspheres (data not shown). We have hypothesized that GJIC of cells in contact with various biomaterials can be used as an index for estimating the biocompatibility of many kinds of biomaterials [5,6,9,11]. In addition, osteoblasts have been reported to communicate with one another *via* GJIC function, and the function is believed to be critical to the coordinated cell behavior necessary in bone tissue development [8,12]. Therefore, effects of these microspheres on the communication of co-cultured NHOst were estimated to consider the relation between this function and the differentiation of NHOst. The FRAP assay revealed that HAp microspheres enhanced the GJIC level of NHOst to 1.8 times as much as that of NHOst alone but others slightly inhibited it, indicating HAp has a potential to enhance homeostasis maintenance function of the NHOst as well as their differentiation. Details of the microspheres effects on GJIC of NHOst will be reported elsewhere [13]. These results indicated that the materials of microspheres affected the differentiation of co-cultured NHOst as well as the diameter of microspheres and their contact with the cells. In addition, microspheres made from HAp, which is a major component of bone tissue and has been shown to have good biocompatibility as bone substitute implants [14], may have the potential to enhance the differentiation of osteoblasts. These results suggest that the estimation of the effects of biomaterials in microsphere form on in vitro cell function may be useful for their in vivo biocompatibility evaluation.

We estimated the effect of sintering, normally used to harden HAp, on the function of NHOst. The estimation revealed that both HAp microspheres enhanced the amount of calcium deposited although the ALP activity of the cells decreased. In addition, when the un-sintered HAp microspheres were incubated with NHOst, the calcium deposition was observed more than sintered HAp. As another index of the differentiation of the NHOst, mRNA expression levels of osteocalcin, which is a well-known protein detected in

Table 1. Effects of a 1-week incubation with pre-coated microspheres on various functions of NHOst.
(Amounts of microspheres = 20 μg/well)

	Control	Polystyrene	Polyethylene	Alumina	Hydroxy Apatite (Sintered)
Diameter (μm)		5.0	6.4	5.1	7.2
The cell number ratio (%)	100.0±5.5	88.2±2.2	92.2±1.3	82.4±2.8	83.0±2.3
Percent ALP activity (activity/proliferation)	100.0±4.7	79.2±5.6	72.7±3.6*	58.2±5.7*	73.8±6.0*
Percent deposited calcium (Calcium percent/proliferation)	100.0±3.7	97.3±4.2	82.3±3.7	90.3±7.8	163.3±18.5*(a

Data are shown as the mean value ± SEM (n = 4 to 22)
* $p < 0.01$, against control group
(a) $p < 0.05$, against NHOst co-cultured with polyethylene and alumina microspheres

differentiated osteoblasts [15], were determined using the RT-PCR technique. Figure 2 shows time profiles of osteocalcin mRNA expression in NHOst cultured with pre-coated PS, PE, alumina, and two kinds of HAp microspheres. As shown in the figure, only the cells co-cultured with sintered HAp microspheres expressed osteocalcin mRNA after a 1-day incubation, while those co-cultured with other microspheres did not express the mRNA. This finding suggests that sintered HAp microspheres have the potential to induce osteocalcin production from NHOst. Neither spontaneous calcium deposition was observed by the incubation of sintered nor un-sintered HAp microspheres without NHOst, so that it is possible that the un-sintered HAp degrade in culture medium with NHOst, resulting in an increase of calcium concentration in the culture medium that enhances the calcium deposition by the NHOst. Therefore, it is suggested that sintered HAp can induce the differentiation of NHOst, and may be a suitable material for inducing osteogenesis rather than un-sintered one.

In conclusion, microspheres made from various materials had an effect on the differentiation of NHOst. The level of the effect varied with the size, amount, and composition of the microspheres. Microspheres made from PS, PE and alumina showed a potential to suppress the proliferation and the differentiation of co-cultured NHOst. On the other hand, microspheres made from HAp, especially sintered HAp, enhanced the differentiation of co-cultured NHOst, and showed their potential to maintain their homeostasis. Estimating the effect of various microspheres on the differentiation of osteoblasts will provide valuable information on the effects of wear debris from artificial hip joints as well as estimating their effects on osteoclast function.

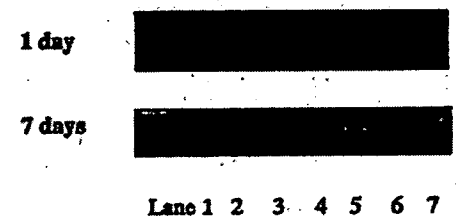

Figure 2. Expression of osteocalcin mRNA extracted from NHOst cultured on various microsphere pre-coated dish.
Lane 1: Collagen-coated culture dish, 2: methanol-treated dish, 3: PS, 4: PE, 5: alumina, 6: un-sintered HAp, 7: sintered HAp.

Acknowledgements

We are grateful for the support of Health and Labor Sciences Research Grants for Research on Advanced Medical Technology, Research on Health Sciences focusing on Drug Innovation and Risk Analysis Research on Food and Pharmaceuticals, Ministry of Health, Labour and Welfare.

References

[1] J.A.Savio III, L.M.Overcamp and J.Black, Clin. Mater., **15**, 101 (1994)
[2] T.R.Green, J.Fisher, J.B.Matthews, M.H.Stone and E.Ingham, J. Biomed. Mater. Res. (Appl. Biomater.), **53**, 490 (2000)
[3] M.C.D.Trindade, D.J.Schurman, W.J.Maloney, S.B.Goodman and R.L.Smith, J. Biomed. Mater. Res., **51**, 360 (2000)
[4] C.Vermes et al., J. Bone. Miner. Res., **15**, 1756 (2000)
[5] R.Nakaoka, T.Tsuchiya, K.Sakaguchi and A.Nakamura, J. Biomed. Mater. Res., **57**, 279 (2001)
[6] M.Nagahata, R.Nakaoka, A.Teramoto, K.Abe and T.Tsuchiya, Biomaterials, **26**, 5138 (2005)
[7] M.M.Levy et al., Bone, **29**, 317 (2001)
[8] A.D.Maio, V.L.Vega and J.E.Contreras, J. Cell. Physiol., **191**, 269 (2002)
[9] R.Nakaoka and T.Tsuchiya, Mater. Trans., **43**, 3122 (2002)
[10] Y.Tabata and Y.Ikada, Adv. Polym. Sci., **94**, 107 (1990)
[11] T.Tsuchiya, J. Biomater. Sci. Polymer Edn., **11**, 947 (2000)
[12] H.J.Donahue, Z.Li, Z.Zhou and C.E.Yellowley, Am. J. Physiol. Cell Physiol., 278, C315 (2000)
[13] R.Nakaoka, S.Ahmed and T.Tsuchiya, J. Biomed. Mater. Res., in press
[14] K.Degroot, Biomaterials, **1**, 47 (1980)
[15] J.Chen, H.S.Shapiro and J.Sodek, J. Bone Miner. Res., **7**, 987 (1992)

A mouse strain difference in tumorigenesis induced by biodegradable polymers

Saifuddin Ahmed, Toshie Tsuchiya
Division of Medical Devices, National Institute of Health Sciences, 1–18-1 Kamiyoga, Setagaya-ku, Tokyo 158-8501, Japan

Received 13 November 2005; accepted 6 February 2006
Published online 10 August 2006 in Wiley InterScience (www.interscience.wiley.com). DOI: 10.1002/jbm.a.30753

Abstract: The use of poly-L-lactic acid (PLLA) surgical implants for repair of bone fractures has gained popularity in the past decade. The aim of this study was to evaluate the *in vivo* effect of PLLA plates on subcutaneous tissue in two mouse strains, BALB/cJ and SJL/J, which have higher and lower tumorigenicity, respectively. Gap-junctional intercellular communication and protein expression of connexin 43 were significantly suppressed, whereas secretion of transforming growth factor-β1 and expression of extracellular matrix, insulin-like growth factor binding protein 3, and cysteine-rich intestinal protein 2 were significantly increased in PLLA-implanted BALB/cJ mice when compared with BALB/cJ controls. Finally, tumors were formed after implantation of cultured cells from the more-tumorigenic BALB/cJ, but not SJL/J, mice into nude mice. © 2006 Wiley Periodicals, Inc. J Biomed Mater Res 79A: 409–417, 2006

Key words: poly-L-lactic acid; gap-junctional intercellular communication; transforming growth factor-β1; connexin 43; nude mice

INTRODUCTION

The morphologic, chemical, and surface electrical characteristics of a biomaterial can influence the extent of the cellular response to an implant,[1,2] but host factors also contribute, so that an identical material implanted in different species[3,4] or at different anatomical locations[5,6] may elicit different degrees of response. Poly-L-lactic acid (PLLA) is a synthetic degradable polymer with good biocompatibility that is widely used clinically for surgical implants and as a bioabsorbable suture material.[7,8] Long-term implants of PLLA produced tumors in rats,[9] and adverse effects were also reported in other animal experiments.[10] All tumors are generally viewed as the result of disruption of the homeostatic regulation of the cell's ability to respond to extracellular signals, which triggers intracellular signal transduction abnormalities.[11] During the transition from the single-cell organism to the multicellular organism, many genes evolved to regulate these cellular functions. One of these genes is the gene coding for a membrane-associated protein channel (the gap junction).[12] Gap-junctional intercellular communication (GJIC) involves two hemichannels or connexons,[13] and each connexon is composed of six basic protein subunits named connexin (Cx), which allow the cell–cell transfer of small molecules. Approximately 20 connexins are known, and they are expressed in a cell- and development-specific manner.[14,15] GJIC also plays an important role in the maintenance of cell homeostasis and in the control of cell growth.[16] Thus, disruption of GJIC has been shown to contribute to the multi-step, multi-mechanism process of carcinogenesis.[17–19] Several tumor-promoting agents have been shown to restrict GJIC by phosphorylation of connexin proteins, such as connexin 43, which is essential in forming the gap junction channel.[20,21] Our previous study revealed that PLLA increased the secretion of transforming growth factor-β1 (TGF-β1), suppressed the mRNA expression of Cx 43, and inhibited GJIC in the early stage after implantation, thus promoting tumorigenesis in BALB/cJ mice.[22] We have hypothesized that the difference in tumorigenic potentials of PLLA is caused mainly by the different tumor-promoting activities of these biomaterials and that TGF-β1 might have an important role in PLLA-implanted BALB/cJ mice. Therefore, in our present experimental approach, we aimed to determine the novel effects of PLLA plates in two mouse strains, BALB/cJ and SJL/J, after long-term implantation. Among mouse strains, the former is a more tumorigenic strain when compared with the later.[23]

Correspondence to: T. Tsuchiya; e-mail: tsuchiya@nihs.go.jp
Contract grant sponsors: Ministry of Health, Labour and Welfare and Japan Health Sciences Foundation

Immune-deficient nude mice, which are highly susceptible to tumorigenicity, were also used in this experiment.

MATERIALS AND METHODS

Animals

Five-week-old female BALB/cJ and SJL/J, and five-week-old male BALB/cAnCrj-nu mice were purchased from Charles River (Japan) and maintained in the animal center according to the NIHS animal welfare guidelines. All mice were fed standard pellet diets and water *ad libitum* before and after PLLA implantation.

Implantation of PLLA

PLLA was obtained from Shimadzu Co. Ltd. as uniform sheets. The implants (size, 20 × 10 × 1 mm^3; Mw, 200,000) were sterilized using ethylene oxide gas prior to use. Sodium pentobarbital (4 mg/kg) was intraperitoneally administered to the mice. The dorsal skin was shaved and scrubbed with 70% alcohol. Using an aseptic technique, an incision of about 2 cm was made; a subcutaneous pocket was formed by blunt dissection away from the incision, and one piece of PLLA was placed in the pocket. The incision was closed with silk sutures. In both strains, controls were obtained by sham operation and subsequent subcutaneous pocket formation. Following surgery, the mice were housed in individual cages. After 10 months, mice from the implanted group were killed, implanted materials were excised, and subcutaneous tissues from the adjacent sites were collected for culture. At the same time, subcutaneous tissues were removed from the sites in the sham-operated controls that correlated with the implant sites. Similar experiments were also performed 1 month after PLLA implantation.[22]

Cell culture of subcutaneous tissues

The subcutaneous tissues were maintained in minimum essential medium (MEM) supplemented with 10% FBS in a 5% CO_2 atmosphere at 37°C.

Giemsa staining

When cells reached confluence in tissue culture dishes, they were fixed and stained with Giemsa solution. Cell morphology was determined under an inverted light microscope.

Western blot analysis

When cells had grown confluent in 60-mm tissue culture dishes, all cells were lysed directly in 100 μL 2% sodium dodecyl sulfate (SDS) gel loading buffer (50 m*M* Tris-HCl, pH 6.8, 100 m*M* 2-mercaptoethanol, 2% SDS, 0.1% bromophenol blue, and 10% glycerol). The protein concentration of the cleared lysate was measured using a micro-plate BCA protein assay (Pierce, Rockford, IL). Equivalent protein samples were analyzed by 7.5% SDS-polyacrylamide gel electrophoresis. The proteins were transferred to Hybond-ECL nitrocellulose membranes (Amersham Pharmacia Biotech UK, Buckinghamshire, UK), and Cx 43 protein was detected by anti-Cx 43 polyclonal antibodies (ZYMED Laboratories, San Francisco, CA). The membrane was soaked with Block Ace (Yukijirushi Nyugyo, Sapporo, Japan), reacted with the anti-Cx 43 polyclonal antibodies for 1 h, and after washes with phosphate-buffered saline (PBS) containing 0.1% Tween20, reacted with the secondary anti-rabbit IgG antibody conjugated with horseradish peroxidase for 1 h. After several washes with PBS-Tween20, the membrane was detected with the ECL detection system (Amersham Pharmacia Biotech UK).

Scrape-loading and dye transfer assay

The scrape-loading and dye transfer (SLDT) technique was performed by the method of El-Fouly et al.[24] Confluent monolayer cells in 35-mm culture dishes were used. After rinsing with Ca^{2+}, Mg^{2+} PBS(+), cell dishes were loaded with 0.1% Lucifer Yellow (Molecular Probes, Eugene, OR) in PBS(+) solution and were scraped immediately with a sharp blade. After incubation for 5 min at 37°C, cells were washed three times with PBS(+), and the extent of dye transfer was monitored using a fluorescence microscope equipped with a type UFX-DXII CCD camera and a super high-pressure mercury lamp power supply (Nikon, Tokyo, Japan).

Enzyme-linked immunosorbent assay

Cells were seeded onto 60-mm dishes. The conditioned medium was collected after centrifugation at 1000 rpm for 2 min. The TGF-β1 levels of the media were measured with commercially available enzyme linked immunosorbent assay (ELISA) kits (R&D Systems, Minneapolis, MN).

DNA microarray analysis

At least 10^7 cells were harvested and frozen in liquid nitrogen. Total RNA was extracted, purified, and assessed for yield and purity, and cDNA probes were synthesized with the Atlas™ Pure Total RNA Labeling System (Clontech) according to the manufacturer's instructions. Hybridization of the ^{33}P-labeled probes to the Atlas Array of Mouse Cancer 1.2 k Array (Clontec 7858–1), on which 1176 cDNAs

of cancer-related genes were spotted, was performed with Atlas™ cDNA Expression Arrays according to the manufacturer's instructions. The phosphor images of hybridized arrays were analyzed with AtlasImage™ (Clontech). Genes that were up- or downregulated more than fivefold relative to the negative controls are discussed.

Determination of tumorigenicity in nude mice

Cultured cells were harvested by trypsinization, and 2×10^6 washed cells suspended in 0.2 mL of PBS were inoculated at a single subcutaneous site into 6–8-week-old nude mice. All mice were examined regularly for the development of tumor.

Soft agar assay

Approximately 100,000 cells per well from each clone were seeded in 2 mL of 0.3% soft agar in culture medium on a solidified basal layer in 6-well tissue culture plates. The plates were cultured for 4 weeks and then stained with *p*-iodotetrazolium violet for 48 h before counting.

Statistical analysis

Student *t* tests were used to assess whether differences observed between the implanted and control samples were statically significant. For comparison of groups of means, one-way analysis of variance was carried out. When significant differences were found, Tukey's pairwise comparisons were used to investigate the nature of the difference. The confidence level was set at 95% for all tests. Statistical significance was accepted at $p < 0.05$. Values were presented as the mean ± SD.

RESULTS

Giemsa staining

Cells with different morphologies formed a slightly crisscrossed pattern in the BALB/cJ control group, whereas cells in the implanted groups of BALB/cJ showed a markedly crisscrossed pattern. The cells were extensively piled up, which decreased contact inhibition, under inverted light microscopy observation and Giemsa staining [Fig. 1(A,B)]. In contrast, the cells of the SJL/J group formed a parallel, flat, confluent monolayer that maintained contact inhibition [Fig. 1(C,D)].

Western blot analysis

We examined the protein expression of the connexin 43 gene and found that the total protein level was significantly decreased in PLLA-implanted BALB/cJ mice when compared with that in BALB/cJ controls (Fig. 2). However, protein expression was decreased in both control and PLLA-implanted groups in SJL/J mice (Fig. 2).

SLDT assay

The SLDT assay was used to assess functional GJIC. GJIC was significantly inhibited in PLLA-implanted BALB/cJ mice when compared with that in BALB/cJ controls (Fig. 3). A significant difference was also observed between the two strains of mice in that the GJIC was lower in SJL/J than in BALB/cJ group (Fig. 3).

ELISA

The secretion of TGF-β1 was significantly increased in PLLA-implanted BALB/cJ subcutaneous tissues in comparison with that from BALB/cJ control mice. On the contrary, secretion of TGF-β1 tended to decrease in the SJL/J implanted mice when compared with that in SJL/J control mice (Fig. 4).

DNA microarray analysis of the four kinds of cells

Expression of the major ECM [fibronectin 1, procollagen VIIIα 1, and osteopontin precursor (OPN)] proteins [Fig. 5(A–C)], insulin-like growth factor binding protein (IGFBP) 3 [Fig. 5(D)], and cysteine-rich intestinal protein 2 (CRIP 2) [Fig. 5(E)] were increased in the PLLA-implanted BALB/cJ mouse cells when compared with that in BALB/cJ control mouse cells. No such difference was observed between SJL/J implanted and control mouse cells.

Tumorigenicity in nude mice

No tumor was formed in PBS(−) injected nude mice [Fig. 6(A)]. Rapid growth of large tumors was observed in nude mice within 2 weeks of injection of cultured cells from PLLA-implanted BALB/cJ mice [Fig. 6(B,C,E,F)]. Nude mice injected with HeLa cells, which served as positive controls, showed slower growth of tumor 4 weeks after cell injection [Fig. 6(D,G)].

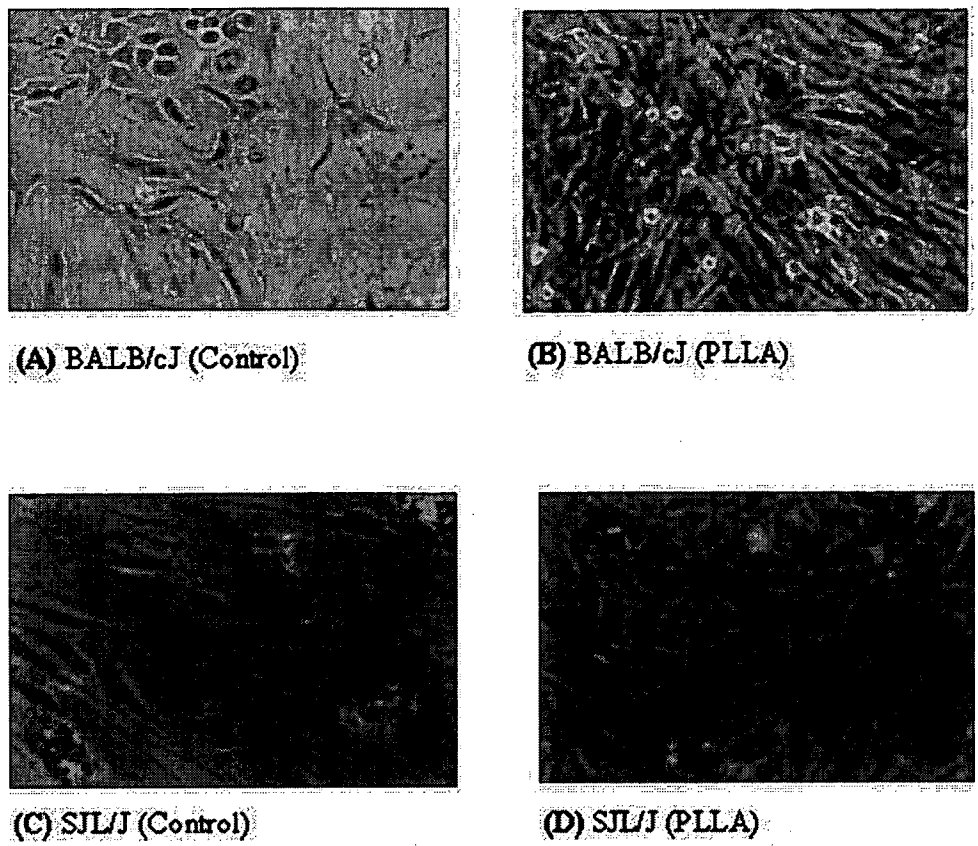

Figure 1. Mouse cell morphology. Three each of both implanted mice and sham-operated controls were killed after 10 months. Results shown are representative of two independent experiments. Inverted light microscopic appearance (magnification ×100) of (A) BALB/cJ (control), (B) BALB/cJ (PLLA), (C) SJL/J (control), and (D) SJL/J (PLLA). [Color figure can be viewed in the online issue, which is available at www.interscience.wiley.com.]

Soft agar assay

These tumor cells did not form a colony in soft agar (data not shown), although HeLa cells did form colonies in soft agar.

Histopathology

Tumor cells from nude mice injected with PLLA-implanted BALB/cJ mouse cells showed monophasic

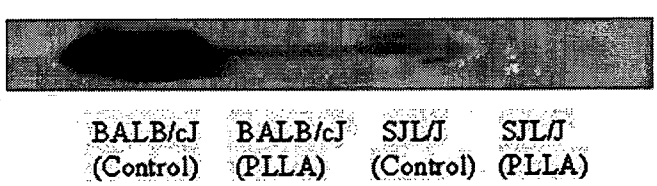

Figure 2. Expression of Cx 43 protein by Western blot analysis. Three each of both implanted mice and sham-operated controls were killed after 10 months. Results shown are representative of two independent experiments. Total protein expression was significantly decreased in PLLA-implanted BALB/cJ mice when compared with that in the control. However, protein expression was decreased in both control and PLLA-implanted groups in SJL/J mice.

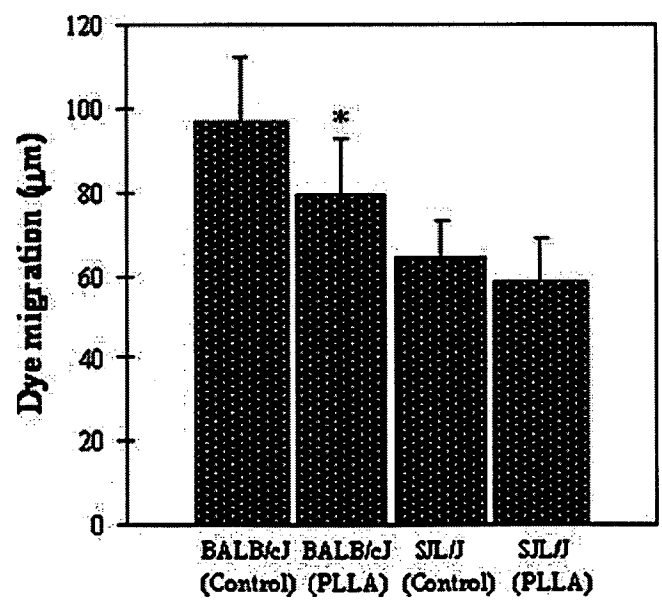

Figure 3. Statistical analysis of SLDT assay. Three each of both implanted mice and sham-operated controls were killed after 10 months. Results shown are representative of two independent experiments. GJIC was found to be significantly inhibited in PLLA-implanted BALB/cJ mice cells when compared with that in BALB/cJ controls. *$p < 0.05$.

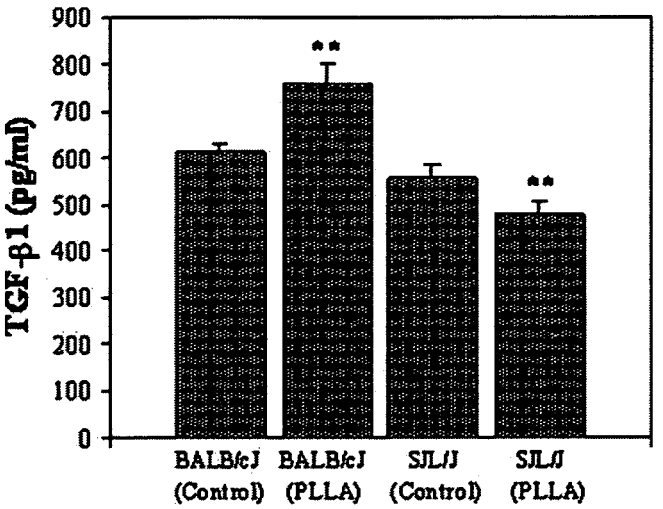

Figure 4. Statistical analysis of TGF-β1 cytokine assay by ELISA. Three each of both implanted mice and sham-operated controls were killed after 10 months. Results shown are representative of two independent experiments. Secretion of TGF-β1 level was significantly increased in PLLA-implanted BALB/cJ mice when compared with that in BALB/cJ controls. On the contrary, in the SJL/J mice, secretion of TGF-β1 tended to decrease in PLLA-implanted mice when compared with that in control mice. $^{**}p < 0.01$.

fibrous synovial sarcoma on H&E and keratin AE1/AE3 staining. Tumor cells with a staghorn pattern [Fig. 7(A)] and a herringbone pattern were identified [Fig. 7(B,C)].

DISCUSSION

Polylactides are bioabsorbable polyesters with wide range of clinical applications. Because it degrades slowly, PLLA has been used as a biomaterial for surgical devices such as bone plates, pins, and screws. It has been reported in different studies that polyetherurethane, nonabsorbable polyethylene, and PLLA produced tumors in rats.[9,10,25–27] Parallel to these studies, here cells with different morphologies formed a crisscross pattern, which thus decreased the contact inhibition in the PLLA-implanted BALB/cJ group [Fig. 1(B)]. We examined the protein expression of Cx 43 to evaluate the actual cause and found that the total level of protein expression was significantly decreased in the PLLA-implanted groups when compared with that in the controls (Fig. 2). In contrast, Cx 43 protein expression was decreased in both control

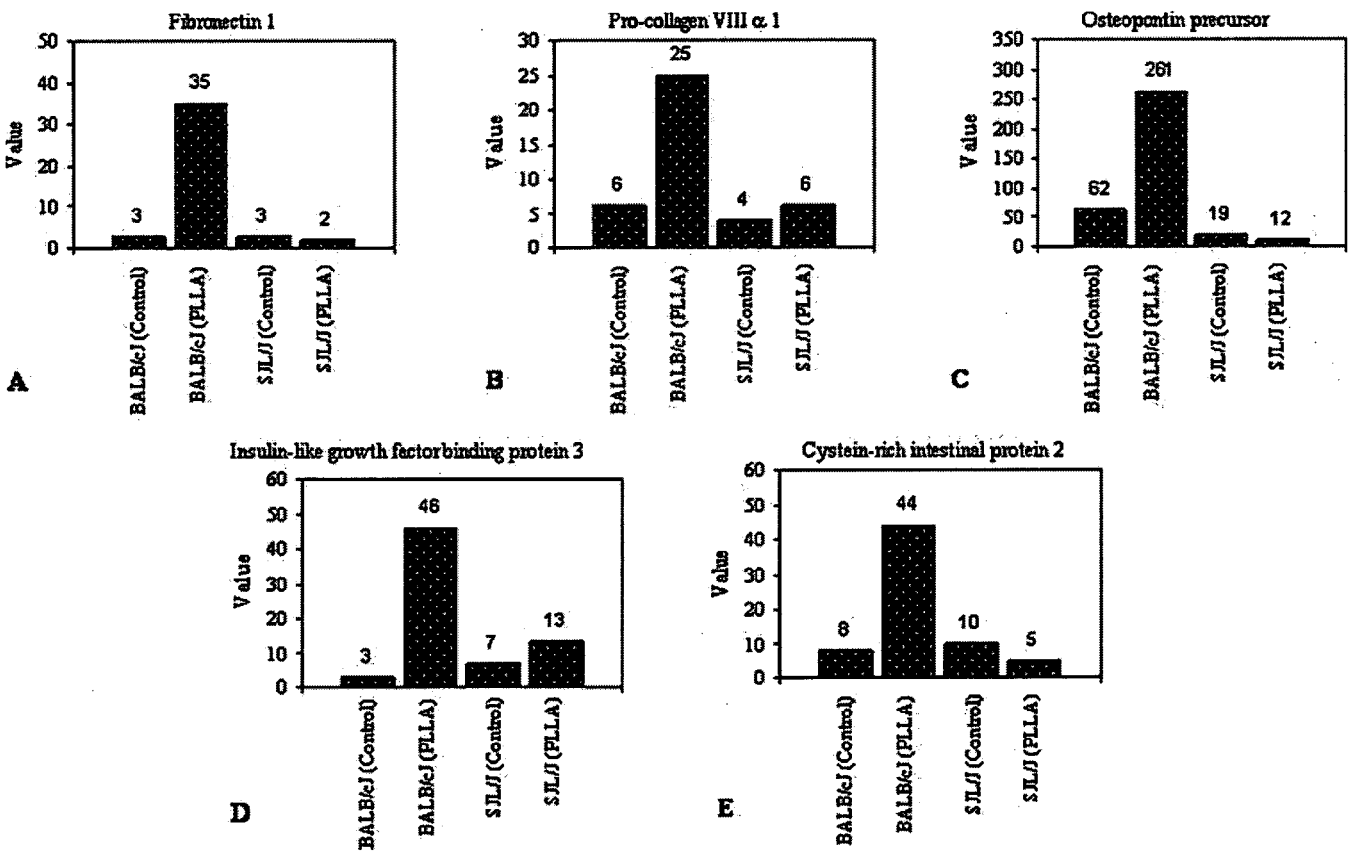

Figure 5. DNA microarray analysis of these four kinds of cells. The expression of (A) fibronectin 1, (B) pro-collagen VIIIα 1, (C) osteopontin precursor (OPN), (D) insulin-like growth factor binding protein (IGFBP) 3, and (E) cysteine-rich intestinal protein 2 (CRIP 2) increased in the cells of PLLA-implanted BALB/cJ mice. Results shown are representative of four independent experiments.

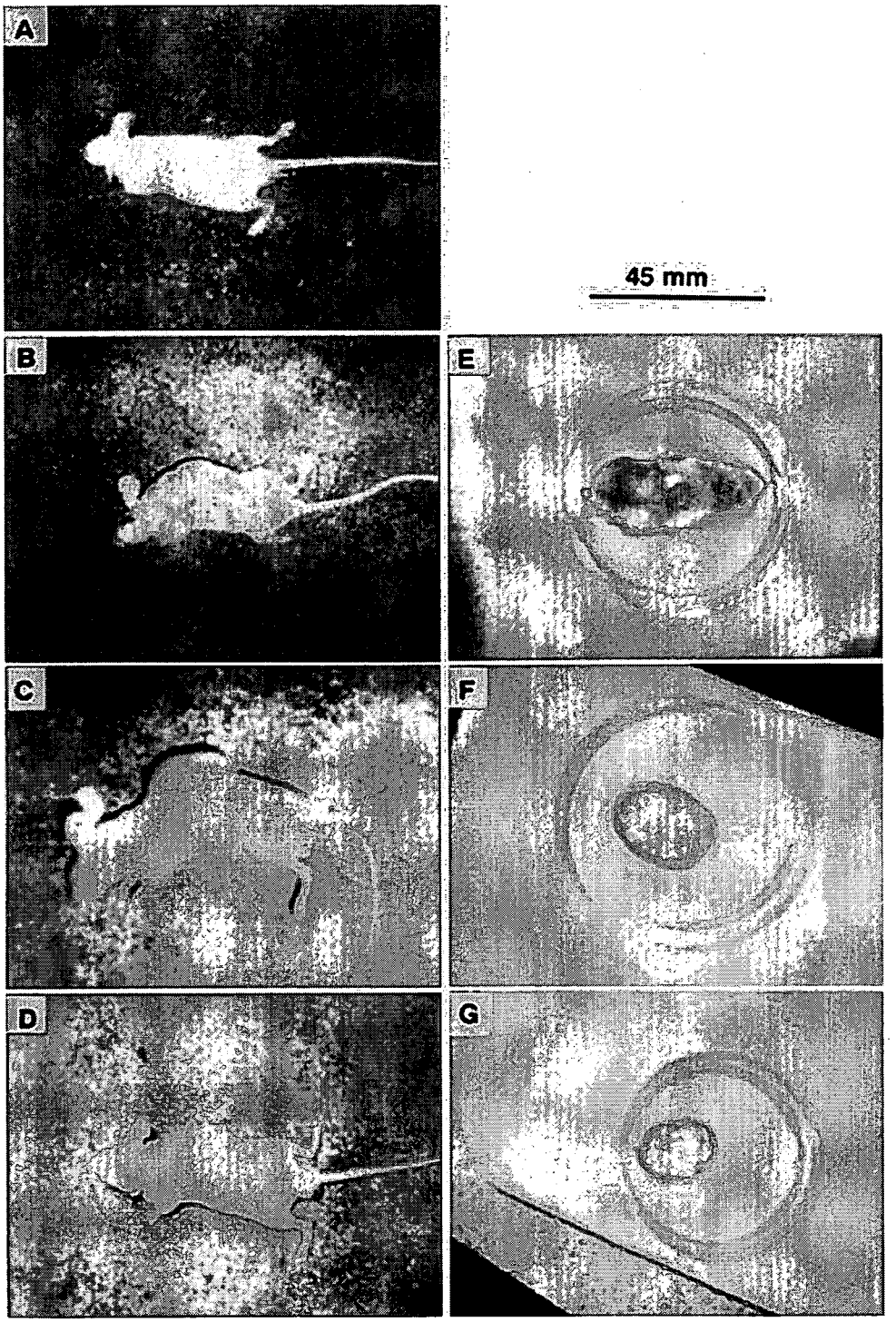

Figure 6. Determination of tumorigenicity in nude mice. (A) No tumor was formed in PBS(−) injected nude mice. (B, C, E, and F) A large tumor growth was observed within two weeks in nude mice injected with cells from PLLA-implanted BALB/cJ mice. (D and G) Tumor growth was observed in nude mice 4 weeks after they were injected with HeLa cells. [Color figure can be viewed in the online issue, which is available at www.interscience.wiley.com.]

and PLLA-implanted groups in SJL/J mice (Fig. 2). We also examined the functional effects on GJIC. In the present study and correlating with our previous report,[22] GJIC was significantly inhibited in PLLA-implanted BALB/cJ mice when compared with that in controls (Fig. 3). Gap junctions are regulated by the post-translational phosphorylation of the carboxy-terminal tail region on the Cx molecule, and hyperphosphorylation of Cx molecules is closely related to the inhibition of GJIC.[28,29] Asamoto et al. reported that tumorigenicity enhanced when the expression of Cx 43 protein was suppressed by the anti-sense RNA of

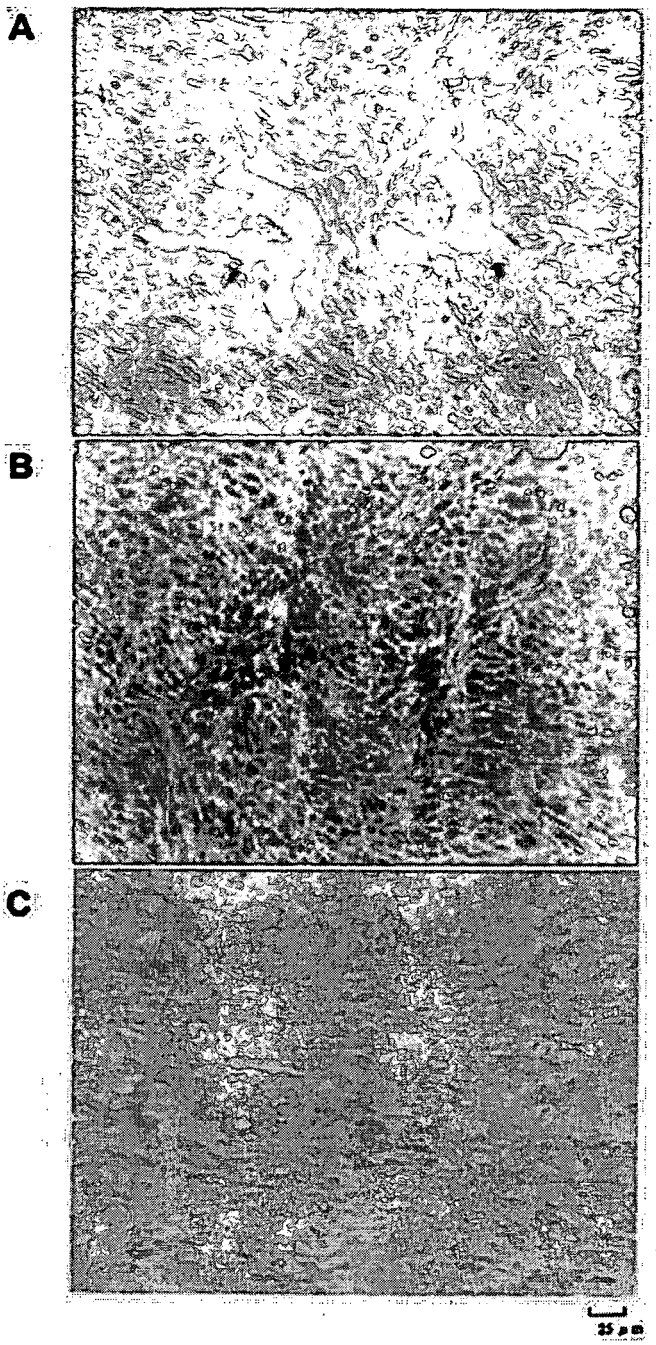

Figure 7. Histopathology. Tumor cells from nude mice injected with cells from PLLA-implanted BALB/cJ mice showed monophasic fibrous synovial sarcoma with H&E and keratin AE1/AE3 staining. (A) Staghorn pattern (H&E), (B) herringbone pattern (H&E), and (C) herringbone pattern (keratin AE1/AE3 staining). [Color figure can be viewed in the online issue, which is available at www.interscience.wiley.com.]

Cx 43.[30] Thus, in our experiment, the impaired GJIC was possibly caused by the suppression of protein expression of Cx 43. Therefore, it is suggested that gap junctions are likely to play a major role in the PLLA-induced tumorigenesis in BALB/cJ mice. But in SJL/J mice, this is not the key factor for tumorigenesis. Another protein may be responsible because Cx 43 protein expression was decreased in both control and PLLA-implanted group of SJL/J mice.

TGF-β1 can impair GJIC function by decreasing the phosphorylated form of Cx 43[31] and can also increase the expression of ECM.[32,33] We estimated the production of TGF-β1 in four kinds of cells. The secretion of TGF-β1 significantly increased in PLLA-implanted BALB/cJ mice cells in comparison with that from BALB/cJ control mice, but TGF-β1 secretion decreased in the SJL/J-implanted group when compared with that in the SJL/J control mice (Fig. 4). Furthermore, by using DNA microarray analysis of these four kinds of cells, expression of the major ECM proteins (fibronectin 1, pro-collagen VIIIα 1, and OPN) and IGFBP 3 was found to be increased in the PLLA-implanted BALB/cJ mice cells (Fig. 5). Several reports have suggested that these proteins could directly cause tumorigenesis.[34–36] Overexpression of CRIP 2, a member of the LIM (characterized by a repeat of a double zinc finger cysteine-rich sequence, CCHC and CCCC) protein family, caused an increase in Th2 cytokine IL-6,[37] and synovial sarcoma cells are reported to produce IL-6 by themselves.[38] Figure 5 shows that IGFBP 3 was highly expressed in the PLLA-implanted BALB/cJ mice cells. In addition, overexpression of IGFBP 3 was associated with poorer prognosis in breast cancer.[36] Therefore, we speculated that overexpression of IGFBP 3 and major ECM proteins directly or indirectly causes tumorigenesis in the PLLA-implanted BALB/cJ mice.

Ten months after implantation of the PLLA plate into BALB/cJ mice, formation of a tissue growth was observed at the implanted site. To determine whether this tissue growth was a tumor or a result of foreign body (PLLA) inflammation, we performed a tumorigenicity assay in nude mice. Rapid growth of a large tumor was observed in nude mice injected with cells obtained from PLLA-implanted BALB/cJ mice (Fig. 6). The histopathologic examination of this tumor disclosed monophasic fibrous synovial sarcoma (Fig. 7). Nude mice injected with HeLa cells as a positive control showed slower tumor growth. However, these PLLA-derived tumor cells did not form a colony in a soft agar assay (data not shown).

We speculated that a protein or regulatory factor other than Cx 43 may play key role in tumorigenesis in PLLA-implanted BALB/cJ mice. In this light, we conclude that overexpression of the regulatory factors such as TGF-β1 and IGFBP 3 caused tumorigenesis in PLLA-implanted BALB/cJ mice. In addition, increased secretion of TGF-β1 suppressed the expression of Cx 43 and inhibited GJIC. Moreover, PLLA increased the expression of ECM, CRIP 2, and OPN. Finally, all these factors in combination promoted tumorigenesis (Fig. 8).

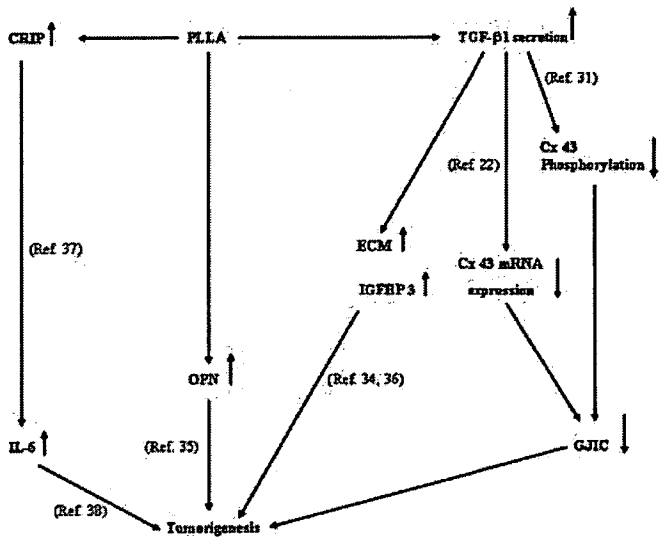

Figure 8. Schematic representation of the pathway of tumorigenesis induced by PLLA in BALB/cJ mice.

References

1. Hayashi T. Interactions between polymers and biosystems: Structure–property relationships in biomaterial polymers. In: Thuruta T, Hayashi T, Kataoka K, Ishihara K, Kimura Y, editors. Biomaterial Applications of Polymeric Materials. Boca Raton, FL: CRC; 1993. pp 17–51.
2. Chesmel KD, Black J. Cellular responses to chemical and morphologic aspects of biomaterial surfaces. I. A novel in vitro model system. J Biomed Mater Res 1995;29:1089–1099.
3. Tang L, Eaton JW. Inflammatory responses to biomaterials. Am J Clin Pathol 1995;103:466–471.
4. Imai Y. Interaction between polymers and biosystem: Biological response to biomedical polymers. In: Thuruta T, Hayashi T, Kataoka K, Ishihara K, Kimura Y, editors. Biomaterial Applications of Polymeric Materials. Boca Raton, FL: CRC; 1993. pp 53–87.
5. Rosengren A, Danielson N, Bjursten LM. Inflammatory reaction dependence on implant localization in rat soft tissue models. Biomaterials 1997;18:979–987.
6. Butler K, Benghuzzi H, Tucci M, Cason Z. A comparison of fibrous tissue formation surrounding intraperitoneal and subcutaneous implantation of ALCAP, HA, and TCP ceramic devices. Biomed Sci Instrum 1997;34:18–23.
7. Kulkarni RK, Pani KC, Neuman C, Leonard F. Polylactic acid for surgical implants. Arch Surg 1966;93:839–843.
8. Craig PH, Williams JA, Davis KW, Magoun AD, Levy AJ, Bogdansky S, Jones JP Jr. A biological comparison of polyglactin 910 and polyglycolic acid synthetic absorbable sutures. Surg Gynecol Obstet 1995;141:1–10.
9. Nakamura T, Shimizu Y, Okumura N, Matsui T, Hyon SH, Shimamoto T. Tumorigenicity of poly-L-lactide (PLLA) plates compared with medical-grade polyethylene. J Biomed Mater Res 1994;28:17–25.
10. Nakamura A, Kawasaki Y, Takada K, Aida Y, Kurokama Y, Kojima S, Shintani H, Matsui M, Nohmi T, Matsuoka A, Sofuni T, Kurihara M, Miyata N, Uchima T, Fujimaki M. Difference in tumor incidence and other tissue responses to polyetherurethanes and polydimethylsiloxane in long-term subcutaneous implantation into rats. J Biomed Mater Res 1992;26:631–650.
11. Trosko JE, Madhukar BV, Chang CC. Endogenous and exogenous modulation of gap junctional intercellular communication: Toxicological and pharmacological implications. Life Sci 1993;53:1–19.
12. Trosko JE, Ruch RJ. Cell–cell communication in carcinogenesis. Front Biosci 1998;3:D208–D236.
13. Falk MM. Biosynthesis and structural composition of gap junction intercellular membrane channels. Eur J Cell Biol 2000;79: 564–574.
14. Evans WH, Martin PE. Gap junctions: Structure and function. Mol Membr Biol 2002;19:121–136. Review.
15. Bruzzone R, White TW, Paul DL. Connections with connexins: The molecular basis of direct intercellular signaling. Eur J Biochem 1996;238:1–27.
16. Loewenstein WR. Junctional intercellular communication and the control of growth. Biochim Biophys Acta 1979;560:1–65.
17. Guthrie SC, Gilula NB. Gap junctional communication and development. Trends Neurosci 1989;12:12–16.
18. Klaunig JE, Ruch RJ. Role of inhibition of intercellular communication in carcinogenesis. Lab Invest 1990;62:135–146.
19. Mesnil M, Yamasaki H. Cell–cell communication and growth control of normal and cancer cells: Evidence and hypothesis. Mol Carcinog 1993;7:14–17.
20. Musil LS, Goodenough DA. Biochemical analysis of connexin43 intracellular transport, phosphorylation, and assembly into gap junctional plaques. J Cell Biol 1991;115:1357–1374.
21. Musil LS, Goodenough DA. Multisubunit assembly of an integral plasma membrane channel protein, gap junction connexin43, occurs after exit from the ER. Cell 1993;74:1065–1077.
22. Ahmed S, Tsuchiya T. A novel mechanism of tumorigenesis: Increased TGF-β1 suppresses the expression of connexin43 in BALB/cJ mice after implantation of PLLA. J Biomed Mater Res A 2004;70:335–340.
23. Brand I, Buoen LC, Brand KG. Foreign-body tumors of mice: Strain and sex differences in latency and incidence. J Natl Cancer Inst 1977;58:1443–1447.
24. El-Fouly MH, Trosko JE, Chang CC. Scrape-loading and dye transfer. A rapid and simple technique to study gap junctional intercellular communication. Exp Cell Res 1987;168:422–430.
25. Tsuchiya T, Hata H, Nakamura A. Studies on the tumor-promoting activity of biomaterials: Inhibition of metabolic cooperation by polyetherurethane and silicone. J Biomed Mater Res 1995;29:113–119.
26. Tsuchiya T. A useful marker for evaluating tissue-engineered products: Gap-junctional communication for assessment of the tumor-promoting action and disruption of cell differentiation in tissue-engineered products. J Biomater Sci Polym Ed 2000; 11:947–959.
27. Nakaoka R, Tsuchiya T, Kato K, Ikada Y, Nakamura A. Studies on tumor-promoting activity of polyethylene: Inhibitory activity of metabolic cooperation on polyethylene surfaces is markedly decreased by surface modification with collagen but not with RGDS peptide. J Biomed Mater Res 1997;35:391–397.
28. Musil LS, Cunningham BA, Edelman GM, Goodenough DA. Differential phosphorylation of the gap junction protein connexin43 in junctional communication-competent and -deficient cell lines. J Cell Biol 1990;111:2077–2088.
29. Lampe PD, Lau AF. Regulation of gap junctions by phosphorylation of connexins. Arch Biochem Biophys 2000;384: 205–215.
30. Asamoto M, Toriyama-Baba T, Krutovskikh V, Cohen SM, Tsuda H. Enhanced tumorigenicity of rat bladder squamous cell carcinoma cells after abrogation of gap junctional intercellular communication. Jpn J Cancer Res 1998;89:481–486.
31. Wyatt LE, Chung CY, Carlsen B, Iida-Klein A, Rudkin GH, Ishida K, Yamaguchi DT, Miller TA. Bone morphogenetic protein-2 (BMP-2) and transforming growth factor-β1 (TGF-β1) alter connexin 43 phosphorylation in MC3T3–E1 Cells. BMC Cell Biol 2001;2:14.

32. Singh LP, Green K, Alexander M, Bassly S, Crook ED. Hexosamines and TGF-β1 use similar signaling pathways to mediate matrix protein synthesis in mesangial cells. Am J Physiol Renal Physiol 2004;286:F409–F416.
33. Kenyon NJ, Ward RW, McGrew G, Last JA. TGF-β1 causes airway fibrosis and increased collagen I and III mRNA in mice. Thorax 2003;58:772–777.
34. Kuchenbauer F, Hopfner U, Stalla J, Arzt E, Stalla GK, Paez-Pereda M. Extracellular matrix components regulate ACTH production and proliferation in corticotroph tumor cells. Mol Cell Endocrinol 2001;175:141–148.
35. Liu SJ, Hu GF, Liu YJ, Liu SG, Gao H, Zhang CS, Wei YY, Xue Y, Lao WD. Effect of human osteopontin on proliferation, transmigration and expression of MMP-2 and MMP-9 in osteosarcoma cells. Chin Med J (Engl) 2004;117:235–240.
36. Rocha RL, Hilsenbeck SG, Jackson JG, VanDenBerg CL, Weng C, Lee AV, Yee D. Insulin-like growth factor binding protein-3 and insulin receptor substrate-1 in breast cancer: Correlation with clinical parameters and disease-free survival. Clin Cancer Res 1997;3:103–109.
37. Cousins RJ, Lanningham-Foster L. Regulation of cysteine-rich intestinal protein, a zinc finger protein, by mediators of the immune response. J Infect Dis 2000;182:S81–S84.
38. Duan Z, Lamendola DE, Penson RT, Kronish KM, Seiden MV. Overexpression of IL-6 but not IL-8 increases paclitaxel resistance of U-2OS human osteosarcoma cells. Cytokine 2002;17:234–242.

Available online at www.sciencedirect.com
SCIENCE DIRECT
Biomaterials
ELSEVIER
Biomaterials 27 (2006) 1437–1443
www.elsevier.com/locate/biomaterials

The effect of hyaluronic acid on insulin secretion in HIT-T15 cells through the enhancement of gap-junctional intercellular communications

Yuping Li[a,1], Tsutomu Nagira[a,b], Toshie Tsuchiya[a,*]

[a]*Division of Medical Devices, National Institute of Health Sciences, 1-18-1 Kamiyoga, Setagaya-ku, Tokyo 158-8501, Japan*
[b]*Japan Association for the Advancement of Medical Equipment, 3-42-6 Hongo, Bunkyo-ku, Tokyo 113-0033, Japan*

Received 28 April 2005; accepted 11 August 2005
Available online 19 September 2005

Abstract

The transplantation of bioartificial pancreas has the potential to restore endogenous insulin secretion in type I diabetes. The bioartificial pancreas is constructed in vitro from cells and a support matrix. Hyaluronic acid (HA) is an extremely ubiquitous polysaccharide of extracellular matrix in the body and plays various biological roles. It has been suggested that high molecular weight (HMW) HA increases in the function of gap-junctional intercellular communications (GJIC) and the expression of connexin-43 (Cx43). To determine whether the function of pancreatic β-cells is affected by gap junctions after HMW HA-treatment, we exposed HIT-T15, a clonal pancreatic β-cell line, in various concentrations of HA for 24 h, and then detected the insulin secretion and content, using an insulin assay kit by ELISA technique. The cellular functions of GJIC were assayed by dye-transfer method using the dye solution of Lucifer yellow. HA-treatment resulted in the enhancement of GJIC function, the increase of insulin release and insulin content. The results obtained in this study suggest that HA-coating increases the insulin secretion of HIT-T15 cells by the enhancement of Cx43-mediated GJIC. The results give useful information on design biocompatibility of HA when is used as a biomaterial for bioartificial pancreas.

Keywords: Hyaluronic acid; Gap-junctional intercellular communications; HIT-T15 cells; Insulin; Bioartificial pancreas

1. Introduction

Type I diabetes is caused by the autoimmune destruction of the β-cells. All patients with type I diabetes require daily insulin shots for the control of glucose levels. However, the insulin therapy cannot inhibit the development of serious chronic complications. The pancreas transplantation has been expected to be the most promising approach toward treating diabetes. The bioartificial pancreas is constructed in vitro from insulin-secreting cells or islets and a support matrix by a tissue engineering method. The frequently used matrix materials are alginate and agar [1,2]. Although bioartificial pancreatic constructs contain insulin-secreting cells entrapped in agar or alginate matrix implanted into the peritoneal cavity of the diabetic patient, mice, and dog, can restore normoglycemia and markedly abate diabetic symptoms, there are important questions in the structural integrity of support matrix, metabolic activity and viability of cells or islets, and late vascular thrombosis [1,2]. Therefore, the new matrix biomaterials, which mimic the functions of extracellular matrix (ECM), need to be researched.

Hyaluronic acid (HA) is an extremely ubiquitous member of the nonsulfated glycosaminoglycan ECM molecule family and is thought to play various biological roles particularly in growth, adhesion, proliferation, differentiation, and cell migration [3,4]. More importantly, the receptor for HA-mediated motility regulates gap-junction

*Corresponding author. Division of Medical Devices, National Institute of Health Sciences, 1-18-1 Kamiyoga, Setagaya-ku, Tokyo 158-8501, Japan. Tel.: +81 3 3700 9196; fax: +81 3 3700 9196.
E-mail address: tsuchiya@nihs.go.jp (T. Tsuchiya).
[1]Present address: School of Life Sciences, Nanchang University of Sciences and Technology, Nanchang, China.

0142-9612/$ - see front matter © 2005 Elsevier Ltd. All rights reserved.
doi:10.1016/j.biomaterials.2005.08.020

channel and connexin-43 (Cx43) expression by its actions on focal adhesions and the associated cytoskeleton [5]. In addition, Park and Tsuchiya [6] have reported that high molecular weight (HMW) HA-coating can enhance the function of gap-junctional intercellular communications (GJIC). The insulin secretion from pancreatic β-cells is a multicellular event depending on their interaction with neurotransmitters and numerous signal molecules carried by blood and also direct interactions between cell–cell and cell–matrix contacts by gap-junctional channels, which mediate exchanges of molecules smaller than 1000 Da, such as ions, small metabolites, and second messengers between adjacent cells. The latter interactions are thought to be crucial regulatory mechanisms of insulin secretion [7–9], and the pharmacological blockade of GJIC markedly decreases insulin release [8]. However, the effects of HMW HA as biomaterials of support matrix on functions of pancreatic β-cells and gap-junctional channel remain unclear.

In the present study, we investigated the effects of HMW HA on the function of GJIC, the expression of Cx43, insulin content, and insulin secretion using HIT-T15 cells in vitro. These results suggest that HMW HA can be used as the biomaterial for the development of a bioartificial pancreas: design biocompatibility of HA depends on the molecular-weight size of HA, and its application method and concentration.

2. Materials and methods

2.1. Materials

Lucifer yellow was purchased from Molecular Probes (Eugene, OR). HA (1680 kDa) and TetraColor ONE (WST-8) were supplied by Seikagaku Industries, Ltd. (Tokyo, Japan). ELISA insulin assay kit was obtained from Morinaga Seikagaku Co. (Yokohama, Japan). Bovine serum albumin (BSA) was obtained from Roche Diagnostics GmbH (Mannheim, Germany). Krebs–Ringer bicarbonate (KRB) buffer (pH 7.4), fetal bovine serum (FBS), and anti-Cx43 were purchased from Sigma Chemical Co. (St. Louis, MO). β-actin antibody was obtained from Cell Signaling Technology Inc. (Tokyo, Japan). Roswell Park Memorial Institute (RPMI) 1640 medium was from Nissui pharmaceutical Co. (Tokyo, Japan). All other chemicals used were obtained from Wako Pure Chemical Industries (Osaka, Japan).

2.2. Preparation of media and culture dishes

The HA polysaccharide was dissolved in distilled water at a concentration of 4 mg/ml. Each of the 35-mm culture dish (Falcon 1008, Becton Dickinson) was coated at a final concentration of 0.01, 0.05, 0.1, 0.5, and 1.0 mg/ml. The HA-coated dishes were dried further under sterile air flow at room temperature for 12 h before use. In order to investigate the effect of HA-addition on the functions of HIT-T15 cells, different media were prepared at a final concentration of 0.01, 0.05, 0.1, 0.5, and 1.0 mg/ml. HA-treatment is performed to cells for 24 h.

2.3. Cells and cell culture

A hamster pancreatic β-cell line, HIT-T15 (HIT-T15 cells, Dainippon Pharmaceutical Co., Japan), was cultured in RPMI 1640 medium containing 10% FBS, 2 mM L-glutamine, 100 IU penicillin-G and 100 μg/ml streptomycin at 37 °C in a humidified atmosphere of 5% CO_2. The subculture cells were seeded at a density of $1.0–5.0 \times 10^5$ cells/ml in multiwell plates or culture dishes. When they reached more than 80% confluence, the cells were used for various studies. Throughout the cell growth period the culture media were replaced every 2 days.

2.4. Measurement of cell viability

To evaluate the affect of HMW HA on cell viability of HIT-T15 cells, HIT-T15 cells (1×10^5) were incubated into the various concentrations of HA-coated 24-well plates, or after the cells were seeded onto 24-well plates and pre-incubated in a 10% FBS/RPMI 1640 medium overnight, the medium was exchanged for 10% FBS/HA/RPMI 1640 medium prepared. After 24 h of HA-treatment, the cell viability was determined by the WST-8 reduction assay, according to the manufacturer's instructions. Control cells received fresh medium without HA.

2.5. Measurement of insulin release and insulin content

HIT-T15 cells were treated as described above. After pre-incubating for 30 min at 37 °C in KRB buffer, no glucose cells were stimulated for 60 min with 11.1 mM glucose in KRB buffer. The medium was collected, centrifuged for 5 min at 3000*g*, and the supernatant was frozen at −80 °C for insulin release assay. Cultures were then extracted for 24 h at 4 °C in acid-ethanol and the extracts also frozen for determination of insulin and protein content. Insulin was determined by ELISA insulin kit with rat insulin as standard, according to the manufacturer's instructions. Protein content was measured by the BCA protein assay reagent kit with albumin as standard (PIERCE). Values of secreted insulin were normalized to protein content.

2.6. Measurement of dye transfer

Gap junction-mediated communication between β-cells regulates the insulin secretion and insulin biosynthesis. Because HMW HA-coating increased the insulin release and insulin content but not HA-added, we tested whether the HA-coating increases the insulin secretion and insulin content have a relationship with gap junctions between HIT-T15 cells. HIT-T15 (5×10^5) cells were exposed to the HA-coated (0.1, 0.25, and 0.5 mg/dish) 35-mm glass coverslip (Ashland, MA) and incubated for 24 h to evaluate dye coupling using Lucifer yellow. The cells were rinsed with phosphate-buffered saline [PBS(+)] containing Ca^{2+}/Mg^{2+}, and 3 ml of PBS(+) containing 1% BSA and 10 mM HEPES (pH 7.4) were added to keep a sufficient pH stability under the microscope. The junctional coupling of HIT-T15 cells was determined by injecting Lucifer yellow into individual cells within monolayer clusters. Injections were performed on a phase-contrast microscope with InjectMan NI2 and microinjector FemtoJet (Eppendorf AG, Germany) using glass micropipette that were filled with a 4% solution of Lucifer yellow CH (MW 457.2) dissolved in 0.33 M lithium chloride, as previously described [11]. An injection pressure of 6.5 psi for 200 ms was used for each injection. The coupling extent was evaluated by counting dye-transferred cells at 2 min after microinjection. There was no leakage of injected dye into the medium.

2.7. Western blot analysis

HIT-T15 cells were grown into the various concentration of HA-coated 100-mm plastic dishes (0.1, 0.25, and 0.5 mg/dish) (FALCON 3003; Falcon) for 24 h, rinsed with Ca^{2+}/Mg^{2+}-free PBS(−) and then lysed in CelLytic™-M lysis/extraction reagent (Sigma). Protein content was measured by the BCA protein assay reagent kit (PIERCE). Samples of total extracts (20 μg protein/lane) were fractionated by eletrophoresis in a 10% sodium dodecyl sulfate polyacrylamide gel electrophoresis (SDS–PAGE). The contents of the gels were transferred to PVDF membranes (Clear Blot Membrane-P). Membranes were saturated for 2 h at room temperature in Block Ace (Dainippon Pharmaceutical Co.,

Japan) and then were incubated with antibodies directed against Cx43 (1:1000) and β-actin (1:1000) as the primary antibody overnight at 4 °C. After repeated rinsing in PBS–Tween, the immunoblots were incubated with a peroxidase-conjugated antibody against rabbit (1:5000) at room temperature for 1 h. Membranes were developed by enhanced chemiluminescence according to the manufacturer's instructions (Amersham Pharmacia Biotech).

3. Results

3.1. Cell viability

In order to evaluate the affect of HMW HA on cell viability, HIT-T15 cells were incubated with HA-coated (0.01, 0.05, 0.1, 0.5, and 1.0 mg/dish) or -added (0.01, 0.05, 0.1, 0.5, and 1.0 mg/ml) for 24 h. After 24 h exposure to HA-added, there was no significant change in the viable HIT-T15 cell number at the low concentration of HA-added ($\leqslant$1.0 mg/dish) compared to control. In contrast, after 24 h of incubation, the cell viability of HIT-T15 cells grown on high concentration HA-coated dishes ($\geqslant$1.0 mg/dish) was significantly less than on low concentration HA-coated and control (Fig. 1). Therefore, all further studies were conducted using low concentration of HA ($\leqslant$0.5 mg/dish).

3.2. Insulin secretion and insulin content

HIT-T15 cells, retain glucose-stimulated insulin secretion, showed an increase in insulin secretion as a function of stimulation. Thus, their insulin output was 2.73±0.36 and 3.90±0.41 pg/μg protein in the base and glucose-stimulation (11.1 mM), respectively (n = 9 dishes from three independent experiments). When these cells were exposed to a low concentration of HA-coating (0.1, 0.25, and 0.5 mg/dish) for 24 h, their insulin secretion was significantly increased in the presence of glucose-stimulation (Fig. 2). However, in contrast, when HIT-T15 cells were incubated with HA-addition for 24 h, the increasing effect was not exhibited. The insulin secretion was without a difference between control and HA-addition (Fig. 2). On the other hand, after acid-ethanol extraction, we found that the insulin content of the HIT-T15 cells grown onto the HA-coated dishes was significantly increased but not HA-added (Fig. 3).

GJIC and Cx43 are thought to be crucial regulatory mechanisms of insulin secretion and insulin content. As described above, HA-coating increased insulin secretion and insulin content of the HIT-T15 cells. In addition, Park and Tsuchiya [6] reported that HMW HA-coating can enhance the function of GJIC in normal human dermal fibroblasts but not HA-addition. Hence, all further studies on the mechanism of insulin secretion and insulin content were conducted using HA-coating.

3.3. Dye transfer

We assessed the function of GJIC using Lucifer yellow by counting the number of dye-transferred cells at 2 min

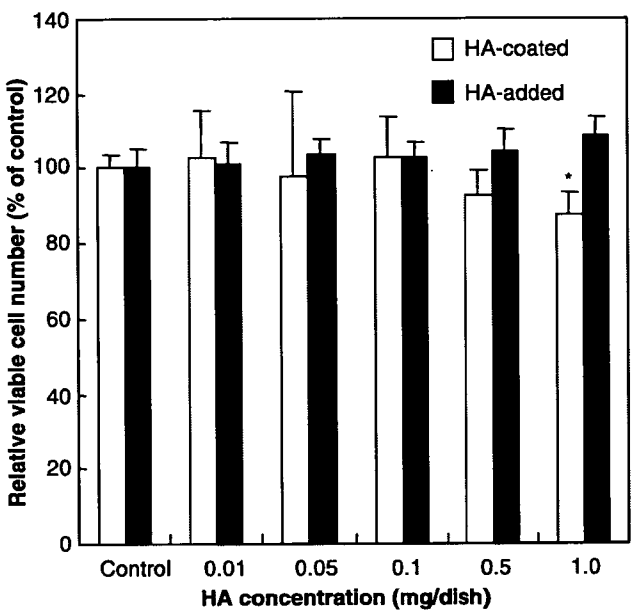

Fig. 1. Concentration-dependent effects of HA-treatment on viability of HIT-T15 cell. After HIT-T15 cells were incubated with HA-coated or HA-added for 24 h, the viable cell numbers of HIT-T15 cell were determined by WST-8 assay as described in methods. Each value denotes the mean±S.D. of three separate experiments. *$P\leqslant0.05$ compared to control under the HA-coated condition.

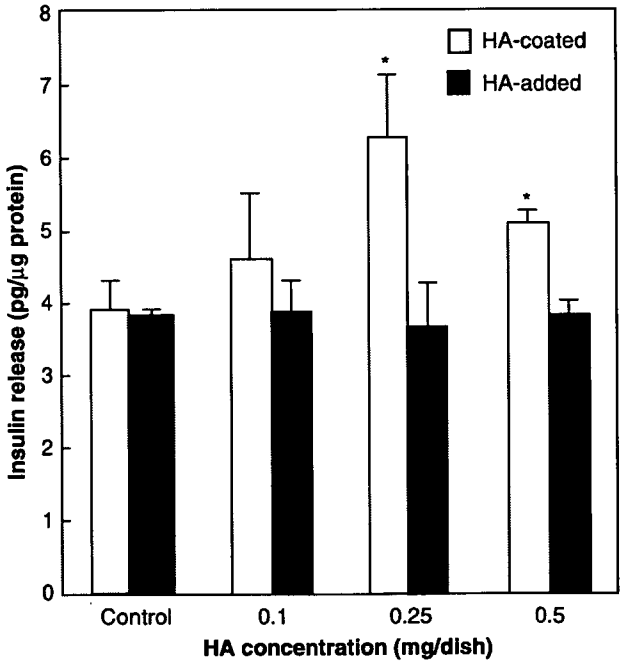

Fig. 2. Insulin secretion from HIT-T15 cells by HA-treatment. HIT-T15 cells were incubated with HA-coating (□) or HA-added (■) for 24 h and then stimulated for 60 min with 11.1 mM glucose in KRB buffer. The released insulin in the spent medium was determined by ELISA insulin kit. Each value denotes the mean±S.D. of three separate experiments. *$P\leqslant0.05$, compared to control in the presence of glucose.

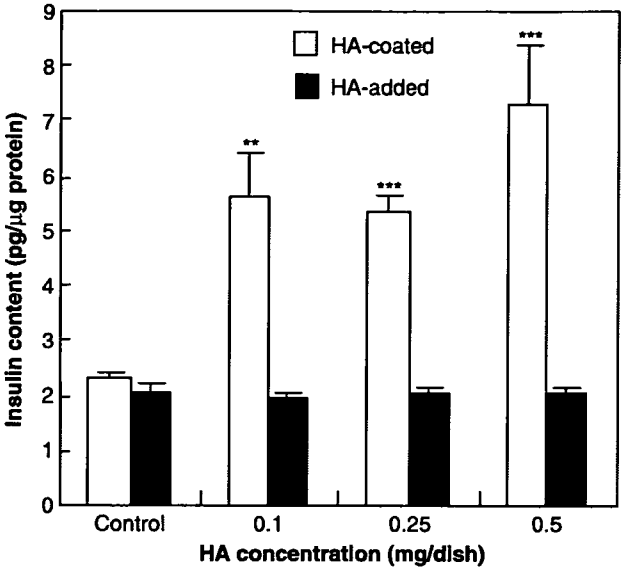

Fig. 3. Insulin content of HIT-T15 cells incubated with HA-coated (□) and HA-added (■). Cells were incubated in the presence of different HA concentrations (0.1–0.5 mg/dish) for 24 h and then stimulated for 60 min with 11.1 mM glucose. The insulin content in the extracts was determined by ELISA insulin kit. Each value denotes the mean ± S.D. of three separate experiments. $^{**}P \leqslant 0.01$ and $^{***}P \leqslant 0.001$ compared to control.

after microinjection. Fig. 4A shows the patterns of dye transfer in HIT-T15 cells treated with HA-coating (0.1, 0.25, and 0.5 mg/dish) for 24 h. Most microinjections led to the intercellular transfer of Lucifer yellow, indicating the frequent coupling of HIT-T15 cells. Under control conditions, microinjection experiments revealed that 47.1% of HIT-T15 cells transferred Lucifer yellow with a limited number (1.5 ± 0.6) of microinjection cells. In HA-coated conditions, almost injected cells (95%) showed Lucifer yellow dye transfer, the number of Lucifer yellow-transferred cells (3.2 ± 1.3, 4.4 ± 1.9, and 4.1 ± 1.9, respectively) was more than that of the control condition ($P < 0.001$) (Fig. 4B), which indicated that GJIC function was activated by the HA-coating.

3.4. Cx43 expression

Cx43 is the 43-kDa member of a conserved family of membrane spanning gap-junction proteins. To provide further evidence that the HA-coating increased the function of GJIC, relative to the levels of actin, comparable levels of immunolabeled Cx43 was detected in 0.1, 0.25, and 0.5 mg/dish of HA-coating cells. Whole cell lysates from HA-coated dish were subjected to SDS–PAGE. Immunoblot analysis was performed with an antibody that specifically recognized Cx43 or β-actin. A Western blot analysis revealed that Cx43 proteins are present in cultured HIT-T15 cells in three forms at 43 kDa region, consisting of a nonphosphorylated form and phosphorylated forms (P1 and P2). HA-coating appeared to induce a greater concentration-dependent increase in all three Cx43 protein levels than control. However, the protein level of β-actin was no different from them (Fig. 5), indicating HA-coating increases the function of GJIC via the expression of Cx43. To account for differences in loading, proteins were both stained with Coomassie blue and immunolabeled for β-actin. The latter staining, which did not change in our experiments relative to that of Coomassie blue (data not shown), was used as an internal standard. These results suggested that HA-coating specifically increased the Cx43 protein but not all cell proteins of HIT-T15 cells.

4. Discussion

The transplantation strategy of bioartificial pancreas is to construct bioartificial tissues in vitro from cells or islets and a support matrix and implant the construct into the body in place of the original. The support matrix must be able to maintain the functions of differentiated cells or contain and/or be able to release appropriate biological signaling information to promote and maintain cell adhesion and differentiation. HA is a high-molecular-mass polysaccharide of support matrix in the body, which is believed to play roles in maintaining various physiological functions including water and plasma protein homeostasis, cell proliferation, cell locomotion, and migration [3]. HA is plentiful, easy to extract and mold into a variety of shape, and biodegradable. It is thus widely used matrix biomaterial for bioartificial tissues [10]. In this study, we investigated whether administration of various concentration of HMW HA influences the viability, GJIC, and insulin secretion of pancreatic β-cells as a matrix biomaterial of bioartificial pancreatic constructs.

Previous study has shown that HMW (310 and 800 kDa) HA-coating (2.0 mg/dish) resulted in low adhesiveness to the cells and the decrease of viability in normal human dermal fibroblasts, because of the change in GJIC functions and induction of various genes including cytokines, adhesion molecules, and growth factors [6,11,12]. In the present study, similar results were obtained. After 12 h, the HIT-T15 cells grown into low concentration HA-coated dishes (0.1, 0.25, and 0.5 mg/dish) and control cells already had attached and confluent but not high concentration HA-coated dishes ($\geqslant 1.0$ mg/dish). We showed that treatment with high concentration of HMW (1680 kDa) HA-coated dose dependently inhibited the viability of HIT-T15 cells. In contrast, there was no difference in viability of HIT-T15 cells between the control and HA-added dishes. These results indicated that among the individual qualities of ECM, the viscosity plays a decisive role. The changes of cell viability by HA-treatment may depend on the cell attachment activity. The difference in cell attachment activity may depend on the surface structure of the coated HA, because the HMW HA-coated surface provides a stable anionic surface that prevents cells attachment at the early time [13]. This result suggests that the molecular-weight size of HA and its

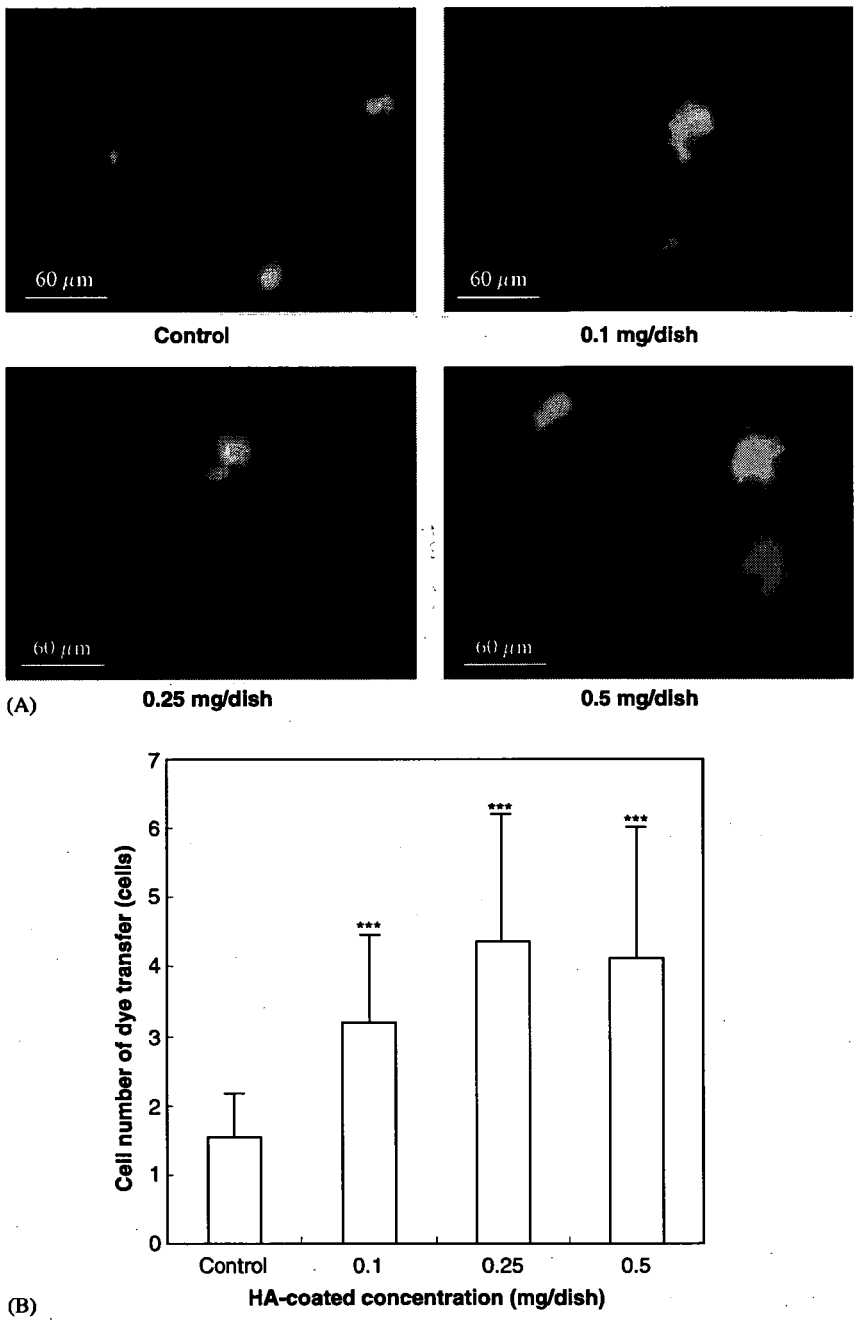

Fig. 4. Concentration-dependent effects of HA-coating on dye transfer in HIT-T15 cells. Cell adherent to glass coverslips were microinjected with 4% Lucifer yellow. Transfer of dye to neighboring cells was assessed by epifluorescence microscopy 2 min later. This is a representative expression of 18 injections per group (A). The number of neighboring cells that received dye was quantified (B). Each value expressed as the mean ± S.D. ($n = 18$). $^{***}P \leqslant 0.001$ compared to control.

application method and concentration are important factors for generating biocompatible tissue-engineered products.

It has been reported that single β-cells (which cannot form gap junctions) show alterations in both basal and stimulated release of insulin, in protein biosynthesis, and in the expression of the insulin gene. The sustained stimulation of insulin release is associated with an increase in β-cells coupling, in the expression of gap junctions by a unique mechanism for direct equilibration of ionic and molecular gradients between nearby cells [14–16]. In this study, we found that the insulin release and insulin content are increased and GJIC activity was enhanced in cultured HIT-T15 cells by low concentration HMW HA-coating in spite of the inhibitory effects on the cell viability in high concentration HA-coating dishes. This finding was consistent with previous reports. The effect of HA may be influenced by the viscosity of HA, the concentration of